Research Square

Preprints are preliminary reports that have not undergone peer review.
They should not be considered conclusive, used to inform clinical practice,
or referenced by the media as validated information.

Long-term Rainfall Variability over Ganga River Basin, India through Clustering and Wavelet Transform Approach

kshitij divyansh

kshitij.divyansh1994@gmail.com

Birla Institute of Technology

vs Rathore

Birla Institute of Technology

Research Article

Keywords:

Posted Date: November 13th, 2026

DOI: https://doi.org/10.21203/rs.3.rs-10986681/v1

License: This work is licensed under a Creative Commons Attribution 4.0 International License.
Read Full License

Long-term Rainfall Variability over Ganga River Basin, India through Clustering and Wavelet Transform Approach

Kshitij Divyansh (Corresponding Author), V.S. Rathore

Department of Remote Sensing and Geoinformatics, Birla Institute of Technology, Mesra, India

Kshitij.divyansh1994@gmail.com, vsrathore@bitmesra.ac.in

Funding: *This research received no specific grant from any funding agency in the public, commercial, or not-for-profit sectors.*

Abstract

Identifying spatiotemporal patterns of rainfall variability is crucial for sustainable water resource management and climate change-adaptive planning. Thus, we attempted to analyze long-term (1984–2024) seasonal and annual CHIRPS daily gridded precipitation data (0.05° × 0.05° resolution) across different agro-climatic zones in the Ganga river basin. For rainfall pattern analysis, we applied hierarchical clustering, discrete and continuous wavelet transform (CWT), and cross-correlation analyses, alongside elevation as a spatial covariate. The study captured the basin's complex hydro-climatic behavior. Clustering delineated three coherent sub-regions of rainfall for winter, pre-monsoon, and post-monsoon seasons, and four for the monsoon season. The Mann–Kendall test and discrete wavelet analysis highlighted modest but discernible upward trends in annual and monsoon rainfall across several zones, overlaid by pronounced inter-annual variability. Notably, the study identified a significant cyclical coherence—particularly in the 2–3-years band—between pre-monsoon and monsoon rainfall, aligning with major climate oscillations such as ENSO and IOD. This relationship underscores the predictive value of pre-monsoon rainfall conditions for anticipating monsoon strength, offering practical implications for seasonal forecasting.

Elevation emerged as a key modulator of rainfall patterns, exhibiting both enhancing and suppressing effects depending on zone and season. For instance, higher altitudes in the Western Himalayan region (Zone 7) enhanced winter and post-monsoon rainfall through orographic uplift, while zones like the Western Plateau and Hills (Zone 6) and Eastern Himalayan region (Zone 9) displayed negative elevation–rainfall gradients due to rain shadow dynamics and moisture depletion at higher elevations. The integrated analysis revealed a nuanced, zone-specific narrative: the rainfed and erosion-prone Central Plateau and Hills (Zone 1), the densely populated and flood-prone Lower Gangetic Plains (Zone 2), the groundwater-stressed yet high-productivity Trans-

Gangetic Plains (Zone 8), and the drought-vulnerable Western Dry region (Zone 10) each illustrate the basin's contrasting rainfall trajectories. Ultimately, this study shows that rainfall variability in the Ganga basin cannot be captured by uniform trends; rather, it is shaped by locally contingent, seasonally distinct, and topographically modulated processes. By revealing dominant periodicities, inter-seasonal connections, and elevation-driven contrasts over four decades. The findings contribute critical insights for hydrological modeling, irrigation planning, and climate-resilient agricultural strategies in one of India's most important and complex river basins.

Introduction

The impact of climate change on hydrological systems is a serious global concern, as water resources are among the most directly affected by shifting climatic conditions (Moradian and Yazdandoost 2021). Precipitation patterns, atmospheric moisture content, and the overall hydrological cycle are tightly coupled to climate variability, making rainfall a critical indicator of ongoing environmental change (Pradhan et al. 2019; Citakoglu and Minarecioglu 2021). The Intergovernmental Panel on Climate Change (IPCC) reports that climatic shifts—both in mean states and variability—are contributing to long-term transformations in hydrology, ecosystems, and water availability (Masson-Delmotte et al. 2022; Sharma et al. 2018; van der Wiel and Bintanja 2021). In South Asia, these impacts are magnified by rapid Himalayan glacier retreat, declining snowfall, and changing meltwater contributions, which directly influence river discharge and groundwater recharge (Hock et al. 2019; Oppenheimer et al. 2019). Reduced precipitation and higher drought risks further threaten water environments and ecological stability across vulnerable regions (Hoegh-Guldberg et al. 2018; Rehman et al. 2022; Tabari 2020).

Climate change is expected to alter rainfall frequency, intensity, and spatial distribution, with many regions projected to experience prolonged dry spells punctuated by extreme rainfall episodes (Martel et al. 2021; Orkodjo et al. 2022). Changes in seasonal onset and shifting atmospheric circulation patterns further compound regional uncertainties (Abbass et al. 2022; Panda et al. 2023). In India, the Indian Summer Monsoon (ISM) remains the dominant climatic driver, contributing most of the annual rainfall between June and September; however, its high spatial and temporal variability often leads to water stress, agricultural disruptions, and large-scale hydrological hazards (Loucks and van Beek 2017). Studies continue to document mixed rainfall trends across the country, with some regions experiencing increasing monsoon rainfall and others showing consistent declines (Praveen et al. 2020). Understanding these spatially diverse rainfall

responses is essential for sustainable water resource planning (Srivastava et al. 2021; Panda and Sahu 2019).

A wide range of statistical and computational tools have been applied to analyze rainfall trends and variability, including the Mann–Kendall test, Hilbert–Huang transform, and machine learning techniques such as artificial neural networks (Reddy and Adarsh 2016; Zerouali et al. 2020; Amato et al. 2020). More advanced multivariate approaches—such as empirical orthogonal functions (EOF), principal component analysis (PCA), and hierarchical clustering analysis (HCA)—have proven effective for identifying meteorologically homogeneous regions and regionalizing hydroclimatic data (Schmidt et al. 2019; Cerón et al. 2020; Zhu et al. 2020). HCA has been widely used to group regions with similar rainfall characteristics, aiding in hydrological modeling and watershed planning, particularly in areas of high spatial variability such as western India (Machiwal et al. 2019). Time-series analysis using wavelet transforms has emerged as a powerful complementary tool for detecting nonstationary temporal behaviors, including periodicities, change points, and multi-scale climate signals within rainfall datasets (Shiau and Chiu 2019; Hochman et al. 2019). Wavelet approaches offer distinct advantages over Fourier-based techniques because they provide simultaneous time–frequency localization (Riabova 2018), and have been successfully applied to assess rainfall periodicity, drought cycles, and meteorological variability (Gupta and Chavan 2021; Yerdelen et al. 2021; Ruwangika et al. 2020).

Given the intensifying impacts of climate change on water resources, there is a growing need to understand long-term seasonal rainfall variability at basin scales to support sustainable hydrology and climate-resilient planning. The Ganga River basin (GRB), one of the largest and most socio-economically important basins in South Asia, exhibits strong climatic and physiographic gradients that shape highly diverse rainfall regimes. To address these complexities, the present study aims to (1) regionalize seasonal precipitation using hierarchical clustering analysis (HCA), and (2) apply continuous wavelet transform (CWT) techniques to evaluate inter-seasonal variability and periodicities across winter, pre-monsoon, monsoon, and post-monsoon seasons. The integration of clustering and wavelet analysis offers a robust methodological framework to identify spatiotemporal rainfall patterns and climate teleconnections critical for hydrological forecasting, water management strategies, and climate adaptation in the Ganga River basin.

Study Area

The Ganga River Basin, one of the major river basins of India was considered for this study. The Ganga River Basin stretches between 21° 53′ N to 31° 46′ N and 73° 38′ E to 89° 09′ E. The area is characterized by vast alluvial plains, and hilly terrain, varies greatly in height(100 - 7800 m above mean sea level). It is around 2525 miles long and has a geographical area of 8,49,000 km². Based on weather patterns and agricultural production, the entire basin is divided into 10 agro-climatic zones (Table 1), with agricultural land making up over 65% of the total area.

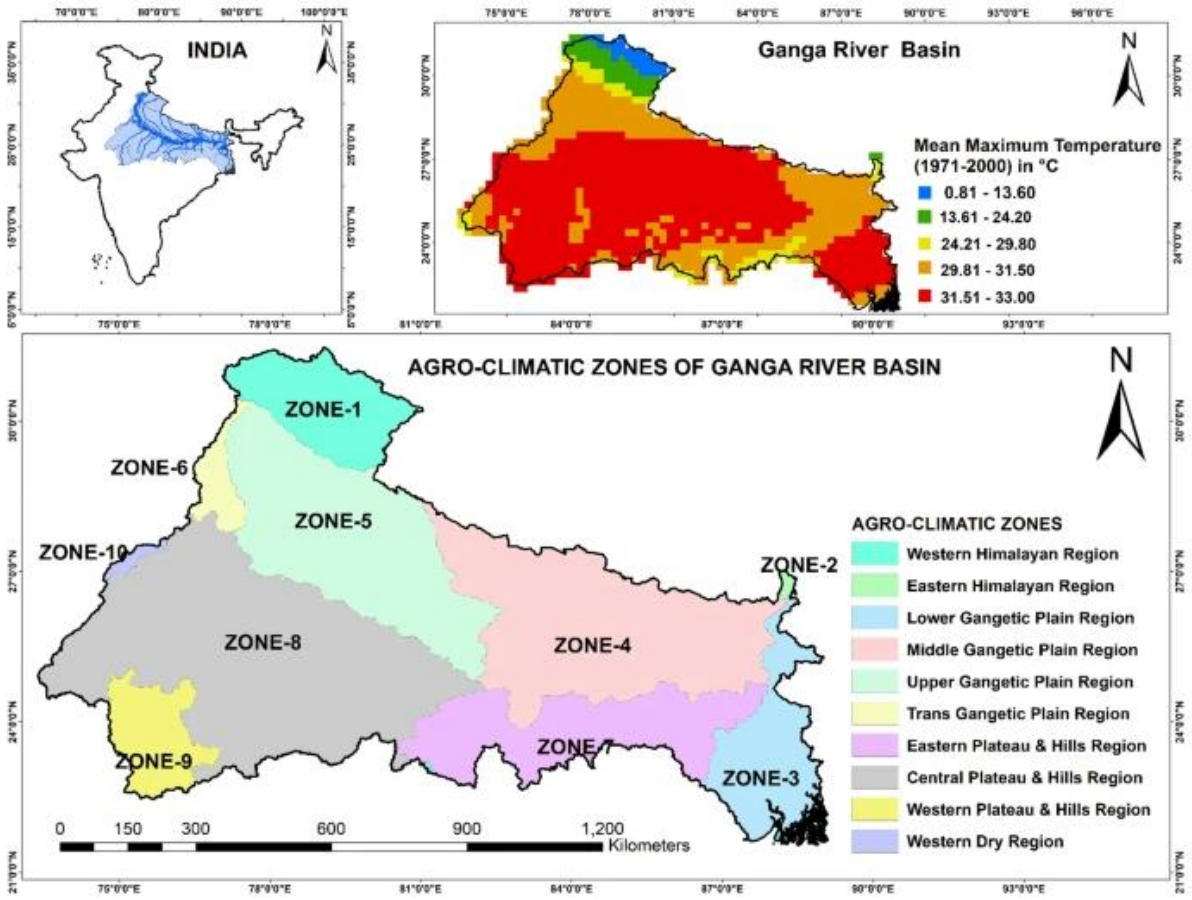


Fig.1: The location map of the study area with different agro-climatic zones.

The area is separated into several agro-climatic zones based on similarities in rainfall, temperature, topography, crops and agricultural systems, and water resources (Fig. 1) Although the GRB has a wide range of land use types, 65.57% of its total area constitutes agricultural land. With alluvial soil covering 52% of the entire area, the basin is the most fertile in India and is abundant in minerals and soil nutrients.

Another notable feature of GRB is its snow and glacier repository, which is crucial for hydropower production and water supplies. The basin has sub-humid to hot and muggy weather during the monsoon season, which lasts from June to September and is characterized by heavy rainfall. The

average annual maximum and lowest temperatures in the basin are around 32.05 °C and 18.44 °C, respectively, with an average annual rainfall of roughly 1059.74 mm. The Alaknanda, Bhagirathi, Yamuna, Gomti, and Betwa rivers are some of the tributaries of the Ganga, which runs for around 2525 km before emptying into the Bay of Bengal.

Data used and Methods

Descriptive statistics, including mean, standard deviation (SD), coefficient of variation (CV), and 5-year moving average were calculated for the analysis of seasonal rainfall. The statistical trend analysis for all four seasons over the basin was also carried out using India Meteorological Department (IMD) seasonal precipitation data. We employed the Mann-Kendall (MK) significance test to discover monotonic increasing and declining trends in the time-series trend analysis of these seasonal data. According to Nisansala et al. (2020), it can be used with time series data that are not normally distributed, including outliers and nonlinear trends. Moreover, it can withstand the effects of time series that are not homogeneous. However, the presence of serial correlation in the time series—which is frequently present in precipitation data—affects the test's sensitivity. The MK test has been employed in numerous research conducted worldwide to analyze long-term rainfall trends (Haktanir and Citakoglu 2014; Nisansala et al. 2020). The MK test details are available in Wang et al. (2020a, b) and Haktanir and Citakoglu (2015). Furthermore, using XLSTAT, SPSS v 17.0, and an Excel spreadsheet, data analysis and HCA were carried out for four rainfall seasons (JJAS). Additionally, we used the wavelet transform in the R 4.0.2 studio to investigate the periodicities in seasonal rainfall. Fig. 2 displays the overall methods used for this investigation.

The rainfall with elevation changes was analyzed using Climate Hazards InfraRed Precipitation with Station data (CHIRPS). The Climate Hazards Center offers precipitation data with a resolution of 0.05°. The worldwide rainfall dataset was intended to enable climate monitoring and early warning systems. It provides precipitation estimates for daily, monthly and annual since 1984 by combining data from in situ stations with satellite Imagery.

Table 1: Distribution of meteorological seasons over India. Source: Moni et al. (2020)

Seasons	Months
Pre-monsoon	March–May (MAM)
Monsoon	June–September (JJAS)
Post-monsoon	October–November (ON)
Winter	December-February (DJF)

The following statistical techniques were used to analyze change breakpoints and precipitation trends:

Mann-Kendall (MK) Test

Several studies have employed the Man Kendall test and the Theil Sen Median Trend test to determine precipitation trends (Burn et al., 2002; Hirsch et al., 1982; Mavromatis & Stathis, 2011; Tabari & Marof, 2011). From 1980 to 2018, the non-parametric statistical MK test (Mann, 1945; Kendall, 1948) is used to examine the detectability of significant trends in time and space. MK is a popular trend identification technique utilized in assessments of severe events (Donat et al., 2013) and precipitation research (Pujol et al., 2007; Pingale et al., 2014; Cooley and Chang, 2021). Since non-parametric tests are less susceptible to outliers, they have been shown to be effective in assessing climate trends (Zilli et al., 2017; Haghtalab et al., 2020). MK compares the null hypothesis—that there is no trend—with the premise that there is either an increasing or declining trend in the time series. At every grid point, the hypothesis is evaluated at three alpha significance levels (α), namely 0.01, 0.05, and 0.10. According to Hirsch et al. (1982), the standardized test statistics Z at each grid point is estimated as follows.

Var is adjusted when there are ties in the sequence of the observation where f_t represents frequency of rank *t* within a tied group. In a time series sequence, a tied group is a set of identical observations, where *n* is the number of years within the record (39).

Theil Sen test for Median Trend

The overall change in precipitation dynamics over the research period is ascertained using this statistical test. This statistical technique, which is non-parametric, is employed to identify patterns in data. It is especially helpful for analyzing datasets with a non-normal distribution or in the presence of outliers since it is resilient to outliers and does not need assumptions about the data's distribution. Henry Theil and Pranab Sen created this method (Sen, 1968; Theil, 1950). The following formula is used to determine each pixel's slope magnitude (Tian et al., 2017; Yang et al., 2019):

$$S_{TS} = \frac{P_j - P_i}{j - i}$$

where P_i and P_j are the Sen's slope and S_{TS} is the corresponding years' precipitation levels. Sen's slope values over 0 indicate a tendency toward higher precipitation, whereas values below 0

indicate a trend toward lesser precipitation. This study was conducted using the R package "wql" (version 1.0.0).

The Mann-Kendall trend test is used to determine the significance of Theil-Sen median slopes. According to Branco et al. (2019), this technique is especially helpful for determining the significance of trends and identifying possible changes in vegetation patterns over time. The Mann-Kendall statistic (S) is computed by adding the signs of the variations in precipitation values across all data point pairings. Its foundation is the relationship between a time series' rankings and sequences. The alternative hypothesis postulates the existence of a monotonic trend, whereas the null hypothesis postulates that the data are independently distributed. The calculated statistics are then compared against critical values obtained from the conventional normal distribution in order to determine the trend's significance (Gilbert, 1987; Kendall, 1948; Mann, 1945). To determine the significance of the estimated trend at the α=0.05 confidence level, we employed the p-value of Kendall's Tau in this investigation.

Cluster Analysis

Several sophisticated approaches, such as cluster analysis, divide components into groups based on the strong correlation between their attributes, such as homogeneous resemblance and other geographical-physical aspects (Zolfaghari et al. 2019). Agglomerative hierarchical clustering (AHC), commonly known as the "bottom-up" approach, was employed for this investigation. This is where all of the recorded observations form clusters and combine to generate a single cluster of related information. This clustering has been applied in a number of recent research (Hu et al. 2019; Jaya et al. 2020), and the results showed that this technique is considerably simpler to apply. Using the clustering approach, Bouguettaya et al. (2015) addressed some significant applications. Using XLSTAT and SPSS v 17.0 software, we computed the AHC and assessed it using the Euclidean distance (Everitt and Dunn 1991) and Ward's technique (Ward & Hook 1963).

$$d_e = [\sum_{i=1}^{n} (Q_{a,i} - Q_{b,i})]^{1/2}$$

where d_e = Euclidean distance; and $Q_{a,i}$ and $Q_{b,i}$ = quantitative component *i* of individuals a and b

The silhouette coefficient (SC), the most used technique, was used in this study to identify the ideal number of clusters. This approach was covered in greater detail by Zhu et al. (2010). Eq. 2 is used to calculate the values of silhouette S(i) for various clusters (Rousseeuw 1987).

$$S(i) = \frac{b(i) - a(i)}{\max[a(i), b(i)]}$$

where $a(i)$ and $b(i)$ are the mean difference of two different clusters.

To verify a correct number of cluster c, averaging of all S(i) values for every c was done to obtain the average silhouette coefficient s(c), $c = 2, 3,..., n-1$ for all objects. After that, a specific digit of cluster c is determined which relates to the topmost value of the average silhouette coefficient.

Continuous Wavelet Transform

In the subject of hydrology, the wavelet transform is a relatively recent technique for analyzing numerous time-series (Sang 2013; Addison 2017). The continuous wavelet transform (CWT) is one of the most used techniques for analyzing periodicity. In order to determine the periodicity of precipitation, CWT edifies → characteristics in multi-temporal scales (Rashid et al. 2015; Addison 2018; Rashid et al. 2015). Furthermore, we require localized frequency variability with temporal information in order to examine dynamic aspects; the Fourier transform (FT) just gives us the global frequency. Therefore, the time domain is converted to the frequency domain using CWT, which only functions as a change of basis with the signal domain (Joshi et al. 2016). It effectively detects the damping oscillation signals and can withstand signal noise. While CWT, according to mathematical definition, employs regular continuous digital convolution that is reached by continuations operation (integration) over our 1D data signal, discrete wavelets transform (DWT) skips the samples throughout the convolution operations. In order to determine the current patterns in monthly, seasonal, and yearly rainfall from 1960 to 2010, Rashid et al. (2015) employed CWT. Wang et al. (2022) provide the CWT details. Eq. (3) is used by Abdourahamane and Acar (2018) to determine CWT.

$$W_f(a,b) = \frac{1}{\sqrt{a}} \int_{-\infty}^{\infty} f(t) e^{ic\left(\frac{t-b}{a}\right)} e^{\frac{t}{a}\left(\frac{t-b}{a}\right)^2} dt$$

where $W_f(a, b)$-wavelet coefficient, a-periodic level of wavelet, b-time-digit, i-imaginary digit, and c-constant.

Additionally, the Morlet wavelet in CWT was used in this work to identify seasonal precipitation periodicity. Because of its complex character, the Morlet wavelet has the obvious benefit of enabling the detection of time-dependent amplitude and phase for various frequencies (Rhif et al. 2019). Jones et al. (2015) calculated the Morlet wavelet using Eq. 4:

$$\widehat{\varphi_0}(SW) = \pi^{1/4} H(\omega) e^{-(s\omega-\omega_0)^{2/2}}$$

where *s*-wavelet stage, ω-frequency, *H(ω)*-Heaviside step function, φ_0-non-dimensional frequency.

However, the pairwise wavelet coherence could essentially explain the periodic strength between and the interdependence with two different features. Wavelet coherence is an approach used for analyzing the degree of coherence in cross wavelet transform with time–frequency space. The detail of wavelet coherence is available in Torrence and Webster (1999). Moreover, the characteristics of the hydrodynamic climate variable can be delineated, with recurrent and periodic patterns followed by certain regular intervals.

RESULTS

Descriptive Statistics of Rainfall

The analysis of seasonal rainfall across the Ganga River basin's agroclimatic zones (1984–2024) reveals a landscape defined by sharp spatial gradients and high temporal volatility. In the Upper and Middle Ganga Plains (Zones 1–2), the monsoon remains the primary hydrological driver, yet it exhibits extreme inter-annual fluctuations. While Zone 1 showed historical monsoon totals ranging from 559mm to 896mm, it recorded a record high of 1389mm in 2019. In contrast, Zone 2 displays the most acute spatial heterogeneity; rainfall peaks at 2797mm in certain regions while dropping to near-zero in others, reflecting the complex transition between the Himalayan foothills and the plains. As the basin extends eastward into the humid and deltaic zones (Zones 7–10), this variability intensifies, with annual totals frequently surpassing 2000mm due to the influence of the Bay of Bengal and intensified monsoon trough activity. Long-term trajectories indicate a basin-wide "wetting" trend, though the magnitude of this increase varies significantly by region. Zones 1 through 4 show a gradual rise in annual precipitation despite a notable drought period in the early 2000s, while the eastern alluvial plains (Zones 5–6) remain more stationary, with Zone 6 showing statistically weak trends due to pronounced annual noise. A significant shift is observed in the lower floodplain (Zone 8), where rainfall has surged since 2000, suggesting a potential realignment of moisture transport pathways. Ultimately, the Ganga basin exhibits a dual hydrological signal: a progressive increase in total annual rainfall coupled with persistent, unpredictable extremes. This combination suggests that while the basin is becoming wetter, its hydrological stability is increasingly compromised by heightened exposure to both wet and dry anomalies presents critical



Fig. 2: Mean rainfall (mm) over Ganga River basin zonally during period 1984-2024

Table 2: Spatial distribution of agroclimatic zones across the Ganga River Basin and their associated long-term precipitation trends and hydrological characteristics

Agroclimatic Region	Zones	Observed Trend	Primary Hydrological Characteristics
Upper & Middle Ganga Plains	1 & 2	Gradually Increasing	High spatial contrast; Himalayan foothill influence; localized extremes (0 to 2797 mm).
Central Alluvial Plains	3 & 4	Gradually Increasing	Marked inter-annual oscillations; historical drought episodes in the early 2000s.
Eastern Alluvial Plains	5 & 6	Stationary to Mild Positive	Influenced by Bay of Bengal systems; Zone 6 shows high variability with no strong long-term trend.
Lower Floodplain	7 & 8	Consistent Upward	Significant moisture shift post-2000; Zone 8 shows intensified monsoon trough activity.
Deltaic Regions	9 & 10	Modest Upward	Highest basin variability; annual totals frequently exceed 2000 mm; high exposure to marine moisture.

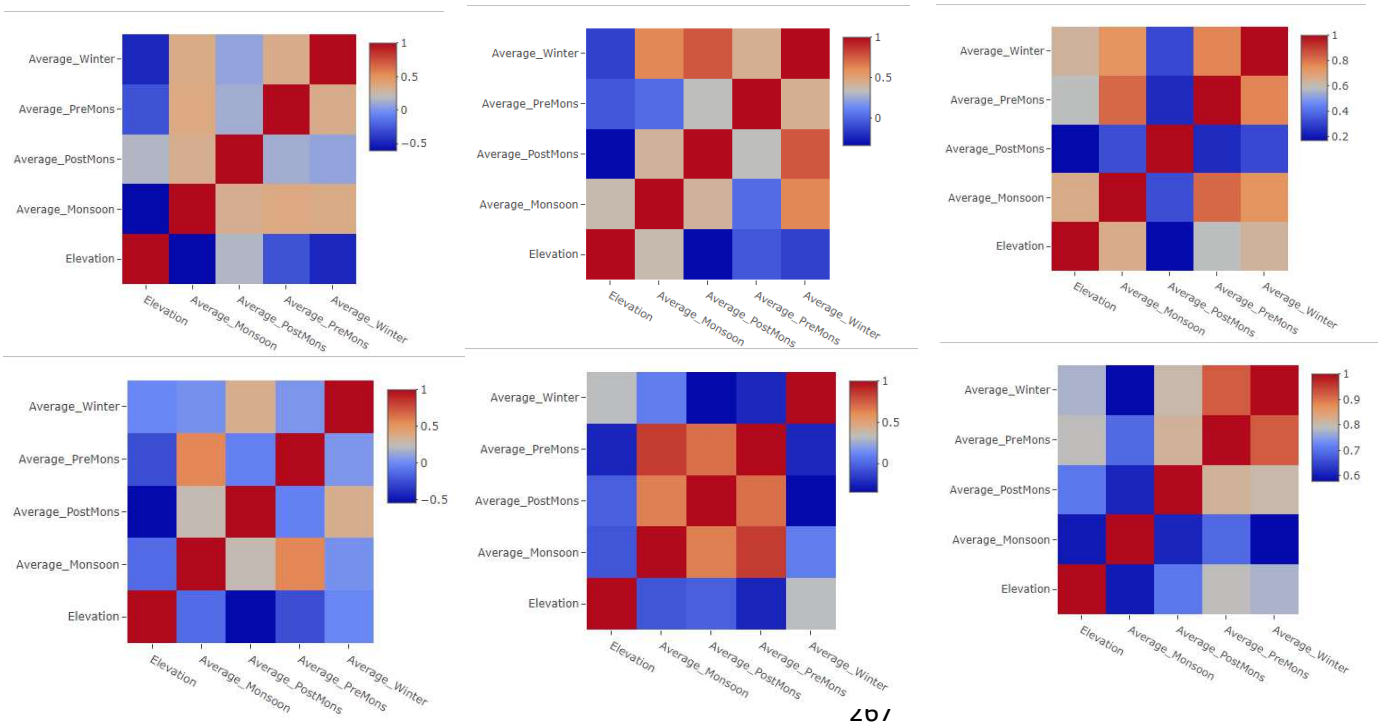
Over the past 40 years, seasonality in the Ganga River basin has undergone a profound reordering, shifting from a regime of predictable, well-distributed rain to one defined by temporal compression and intensified intra-seasonal volatility. While the Indian Summer Monsoon (ISM) still contributes roughly 80% of annual precipitation, the "rainy season" has effectively shortened; a significant decline in the total number of rainy days has been offset by a rise in high-intensity, short-duration extreme events, particularly in the Upper mountainous regions and the Eastern Delta. This compression is accompanied by a breakdown of traditional "lean" season patterns, where pre-monsoon and winter rainfall have become increasingly erratic—showing a notable decrease in the central alluvial plains—while the late-monsoon period (September) exhibits unexpected surges in moisture transport. Consequently, the basin's seasonality is no longer characterized by steady hydration but by a "pulsing" hydrology, where longer, more severe dry spells are interrupted by violent clusters of rainfall, fundamentally disrupting the agricultural calendars and natural recharge cycles that have stabilized the region for centuries.

263

264

265 **Precipitation Trend–Elevation Analysis**

266



267

268

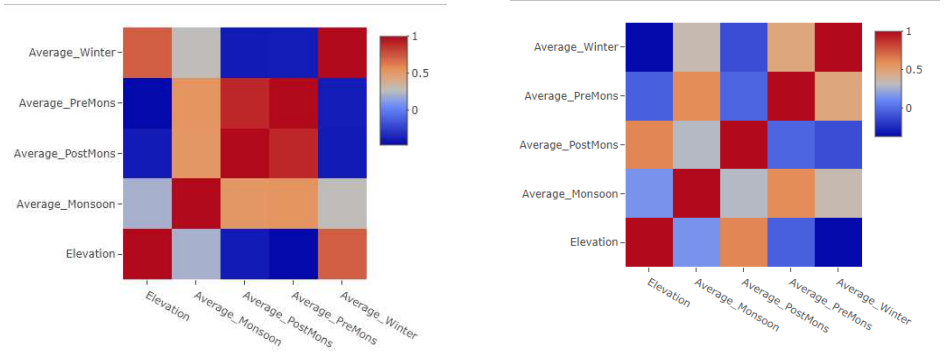
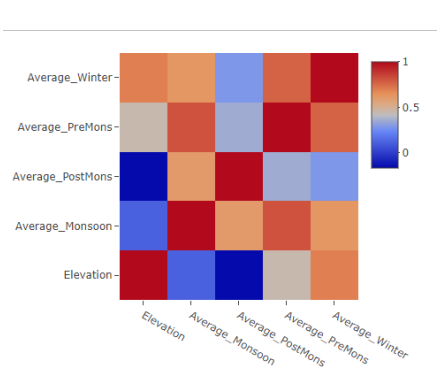
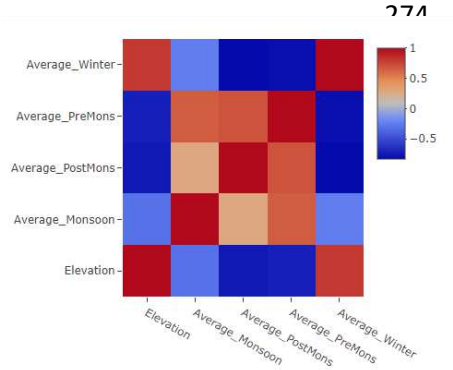


Fig 3: Correlation matrix for seasonal precipitation-elevation in the Ganga River basin.





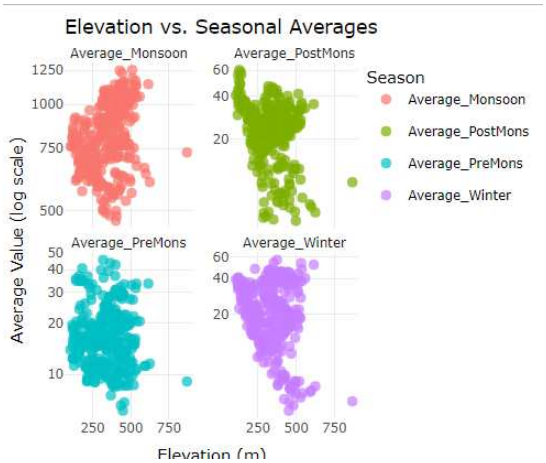
Precipitation-Elevation Dynamics and Seasonal Interconnectivity

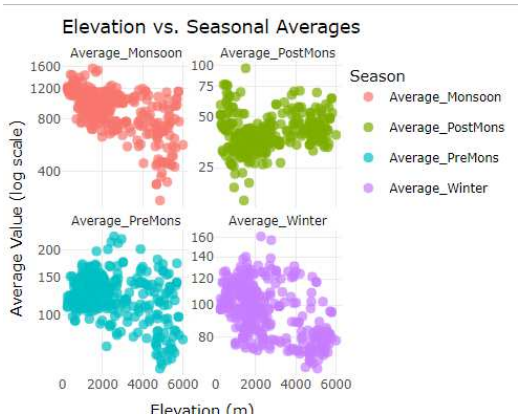
The relationship between elevation and precipitation across the Ganga River basin's ten agroclimatic zones is characterized by non-linear orographic modulation and distinct seasonal decoupling (Fig. 3). Analysis of the 1970–2020 IMD dataset indicates that while winter, pre-monsoon, and post-monsoon precipitation generally scale with elevation, the monsoon season exhibits an inverse relationship. In the high-altitude reaches of the Upper Ganga (Zones 1–2), enhanced orographic lifting drives higher winter and transitional rainfall; however, monsoon totals diminish with altitude due to moisture depletion and rain-shadow effects. Long-term trend estimates (Table X) reveal a non-significant decreasing tendency across all seasons (mean $p=0.3724$), suggesting that topographic control over spatial distribution remains more dominant than temporal shifts. These results corroborate findings by Yao et al. (2016) and Hu et al. (2019), affirming that in Himalayan-fed basins, elevation acts as the primary determinant of rainfall heterogeneity, outweighing long-term secular trends. Correlation heat maps further elucidate the complex interplay between elevation and inter-seasonal moisture pathways. A robust positive association between pre-monsoon and monsoon rainfall in Zones 1, 2, 6, and 7 suggests that early-season convective activity serves as a precursor to monsoon strength, likely modulated by large-scale drivers such as ENSO and the IOD. In the lower floodplain and deltaic zones (Z8, Z9), positive correlations between the monsoon and post-monsoon periods indicate that residual atmospheric instability frequently extends the retreating monsoon phase. Conversely, winter rainfall remains largely independent of tropical monsoon dynamics, showing weak or negative correlations across the basin (specifically in Zones 1, 4, and 6), as it is governed by Western Disturbances. These spatial contrasts—where elevation negatively correlates with monsoon

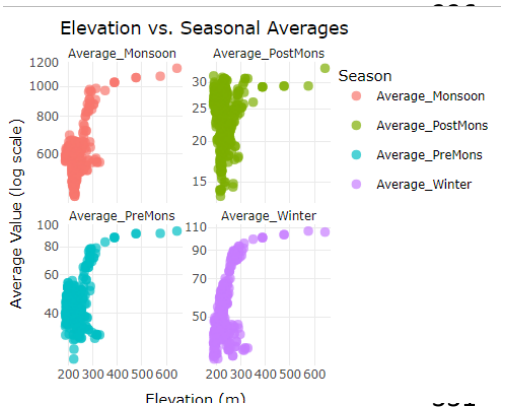
intensity but positively with winter systems—underscore a topographically fragmented rainfall regime that requires zone-specific strategies for hydrological modeling and climate adaptation.

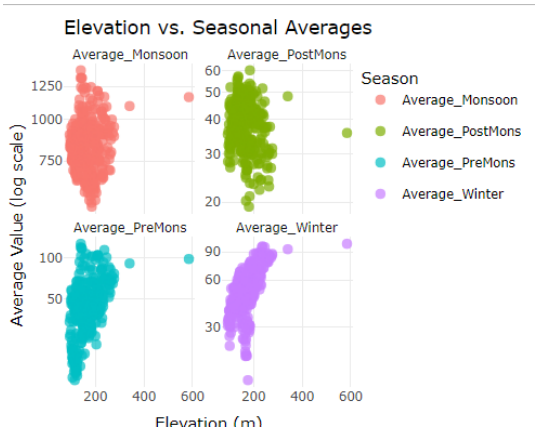
Cluster Analysis of Rainfall-Elevation Gradients

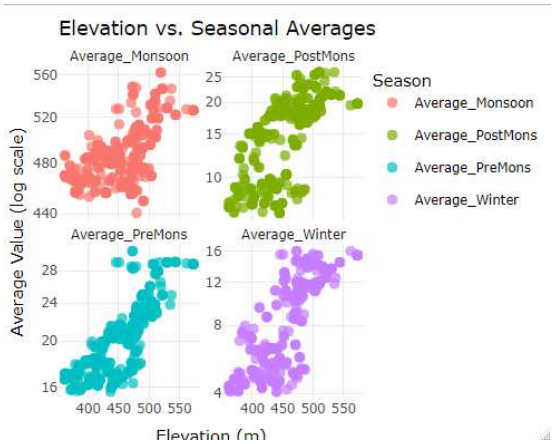
The cluster analysis of seasonal rainfall relative to elevation reveals a distinct bifurcation in the Ganga River basin's hydrological response, primarily driven by orographic processes and regional moisture convergence. Cluster 1 (Zones Z1–Z4), encompassing the Upper and Middle Ganga Plains and the Himalayan foothill belt, is characterized by a generally positive orographic gradient. In Zones Z1 and Z2, monsoon rainfall scales with altitude due to enhanced mechanical uplift and moisture convergence, though winter rainfall conversely declines as high-altitude cooling limits atmospheric water-holding capacity (Yao et al., 2016). Zone Z3 exhibits the most robust positive correlation, where even moderate elevation gains significantly amplify both monsoon and winter totals. This intensification, further reinforced in Z4, underscores the dominant role of orographic lifting in moisture extraction within the northern basin (Bookhagen and Burbank, 2010). Interestingly, even the low-relief Zone Z5 maintains this sensitivity, showing measurable increases in pre-monsoon and transitional rainfall at slightly higher altitudes, indicating that micro topographic variations are sufficient to trigger convective activity.

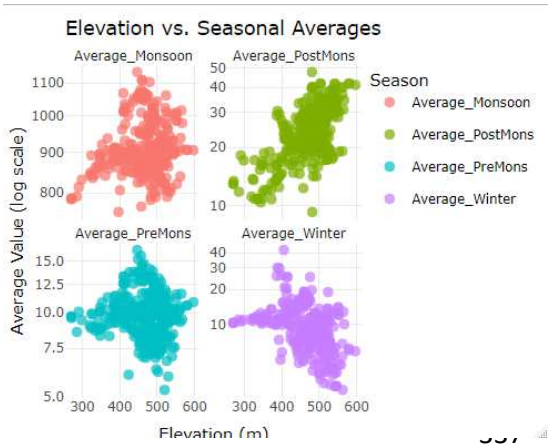


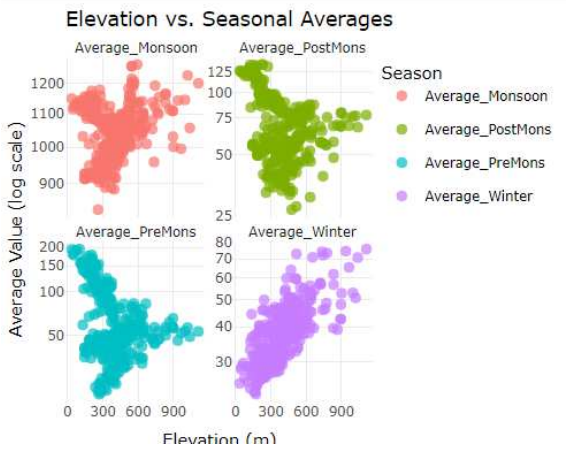


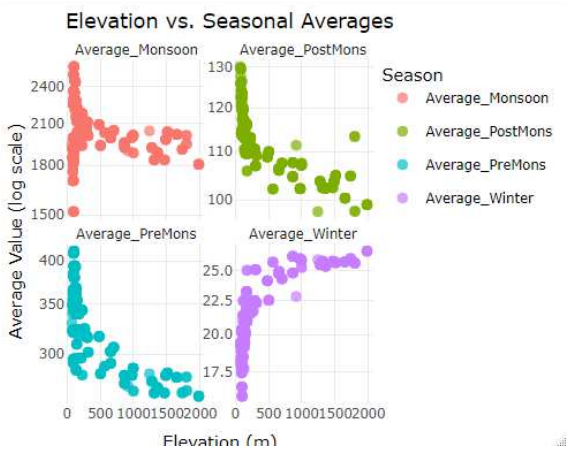

Elevation vs. Seasonal Averages
Average_Monsoon
Average_PostMons
Average_PreMons
Average_Winter
Season
Average_Monsoon
Average_PostMons
Average_PreMons
Average_Winter
Average Value (log scale)
Elevation (m)


Elevation vs. Seasonal Averages
Average_Monsoon
Average_PostMons
Average_PreMons
Average_Winter
Season
Average_Monsoon
Average_PostMons
Average_PreMons
Average_Winter
Average Value (log scale)
Elevation (m)


Elevation vs. Seasonal Averages
Average_Monsoon
Average_PostMons
Average_PreMons
Average_Winter
Season
Average_Monsoon
Average_PostMons
Average_PreMons
Average_Winter
Average Value (log scale)
Elevation (m)


Elevation vs. Seasonal Averages
Average_Monsoon
Average_PostMons
Average_PreMons
Average_Winter
Season
Average_Monsoon
Average_PostMons
Average_PreMons
Average_Winter
Average Value (log scale)
Elevation (m)


Elevation vs. Seasonal Averages
Average_Monsoon
Average_PostMons
Average_PreMons
Average_Winter
Season
Average_Monsoon
Average_PostMons
Average_PreMons
Average_Winter
Average Value (log scale)
Elevation (m)


Elevation vs. Seasonal Averages
Average_Monsoon
Average_PostMons
Average_PreMons
Average_Winter
Season
Average_Monsoon
Average_PostMons
Average_PreMons
Average_Winter
Average Value (log scale)
Elevation (m)

338

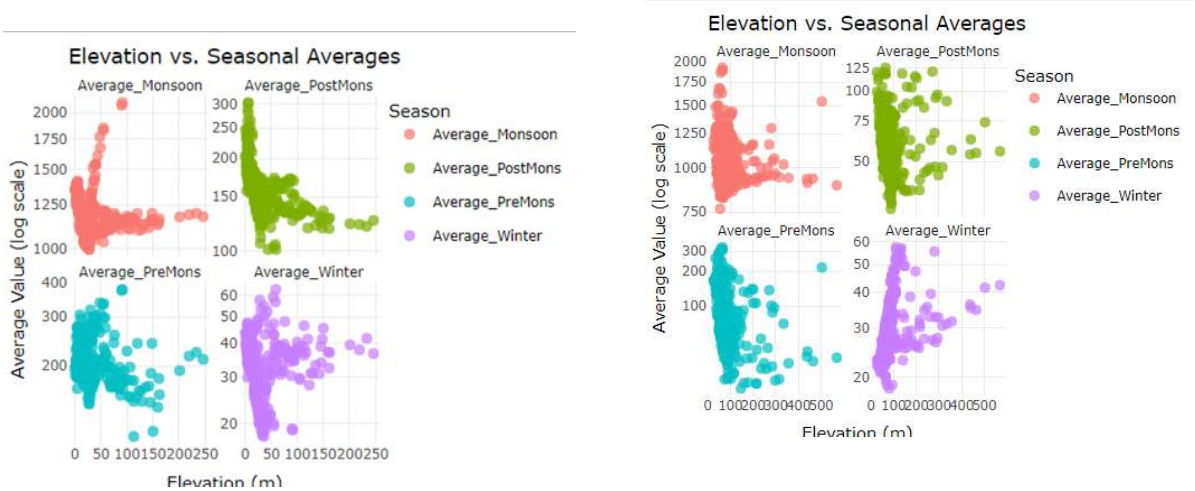


Fig 4: Cluster Analysis of Seasonal Mean Precipitation – Elevation inter relationship in Ganga River basin zonally for the period of 1984-2024.

In contrast, Cluster 2 (Zones Z6–Z10), representing the eastern alluvial plains and deltaic regions, transitions toward a mixed or strongly inverse elevation-rainfall relationship. While Z6 and Z7 show transitional characteristics—with localized increases in winter and post-monsoon rainfall—a definitive shift occurs in the eastern floodplain and delta (Zones Z8–Z10). In these regions, a significant inverse gradient is observed, where monsoon and post-monsoon precipitation are concentrated at the lowest elevations. This pattern reflects the dominance of deep alluvial moisture convergence and the influence of maritime air masses from the Bay of Bengal, which lose intensity as they ascend toward inland upland terrain (Ghosh et al., 2019). The sharp decline in rainfall at higher elevations in Z10 further highlights this deltaic "bottom-heavy" moisture distribution. Collectively, these clusters demonstrate that the basin's topography exerts a non-uniform control, where elevation acts as an intensifier in the northwest but transitions into a limiting factor for moisture availability in the humid southeast.

Table 3 : Regional clustering of agroclimatic zones within the study domain, detailing relationship gradients and primary physical driving mechanisms.

Cluster Group	Representative Zones	Relationship Type	Primary Physical Mechanism
Northern/Western Foothills	Z1, Z2, Z3, Z4	**Positive Gradient**	Orographic uplift; mechanical moisture convergence.

Cluster Group	Representative Zones	Relationship Type	Primary Physical Mechanism
Transitional Plains	Z5, Z6, Z7	**Mixed/Weak Positive**	Micro topographic convective triggers; seasonal decoupling.
Eastern Floodplain & Delta	Z8, Z9, Z10	**Negative Gradient**	Alluvial moisture pooling; maritime influence; altitude-driven depletion.

The synthesis of 40-year temporal trends and elevation-driven spatial clusters reveals a basin in a state of accelerated hydrological transition. While the elevation clusters establish the "geographical blueprint"—where the northern foothills (Z1–Z4) act as orographic intensifiers and the eastern delta (Z8–Z10) serves as a low-lying moisture sink—the long-term trends indicate that climate change is amplifying these existing dynamics.

Table 4 : Interactions between elevation gradients and 40-year precipitation trends across regional clusters, and their resulting hydrological outcomes.

Cluster Region	Elevation Gradient	40-Year Trend Interaction	Hydrological Outcome
Northern Foothills (Z1–Z4)	**Positive** (Rain increases with altitude)	Increasing inter-annual extremes and record highs (e.g., 2019).	**Orographic Intensification:** High risk of cloudbursts and rapid runoff.
Transitional Plains (Z5–Z7)	**Mixed/Stationary**	Statistically weak trends; high annual "noise."	**Stagnant Dynamics:** Relative stability but prone to unpredictable "dry/wet" shifts.
Eastern Delta (Z8–Z10)	**Negative** (Rain peaks at lowest points)	Marked increase in moisture post-2000; high variability.	**Alluvial Loading:** Increased flood frequency in low-lying deltaic sinks.

In the high-elevation northern zones, the positive orographic gradient is becoming more volatile; the "wetting" trend observed over four decades is manifested not as steady rain, but as high-intensity pulses that overwhelm the steep terrain, increasing the risk of flash floods. Conversely,

in the eastern deltaic regions, the inverse elevation gradient is being reinforced by intensified moisture transport from the Bay of Bengal, where the lowest-lying floodplains (Zones 9 and 10) are receiving even higher concentrations of rainfall compared to their inland counterparts. This suggests that the Ganga River basin is moving toward a dual-polarized state: topography is no longer just distributing rainfall, but is actively funneling increased atmospheric moisture into specific "hotspots"—the Himalayan foothills and the deltaic floodplains—thereby exacerbating the spatial heterogeneity of water-related risks across the basin.

Spectral Periodicities and Wavelet Coherence

Continuous Wavelet Transform (CWT) and cross-wavelet spectral analysis (Morlet wavelet) reveal a multi-scale periodic architecture in the Ganga River basin's rainfall. Dominant oscillations are concentrated within the 2–4 year ENSO band, the 4–8 year ENSO–IOD interaction band, and a lower-frequency 8–16 year decadal band (Torrence and Compo, 1998). Significant high-power regions ($p < 0.10$)—demarcated by white contours in the wavelet scalograms (Fig…)—identify periods of synchronized oscillations between monsoon and pre-monsoon rainfall. This synchronization suggests that pre-monsoon convective anomalies serve as a precursor to monsoon intensity, likely modulated by the phase of the El Niño-Southern Oscillation (ENSO). Furthermore, intermittent coherence between monsoon and post-monsoon phases indicates that residual moisture and late-season upper-air circulation patterns frequently extend the influence of the monsoon into the withdrawal period (Krishnamurthy and Goswami, 2000; Pai et al., 2020).In contrast, winter rainfall displays weak and highly sporadic coherence with tropical-monsoon-dominated seasons, underscoring a fundamental synoptic decoupling. While the monsoon and transitional seasons are governed by tropical dynamics (ENSO/IOD), winter precipitation is primarily controlled by mid-latitude Western Disturbances (Dimri et al., 2015). The reliability of these signals is validated by the Cone of Influence (COI), which filters out boundary-effect artifacts, leaving the central scalogram zones to highlight the most robust oscillatory signals. These findings align with similar multi-scale studies in Asian monsoon basins (Han et al., 2021; Li et al., 2021), confirming that while global climate modes exert a dominant control over the basin's wetting and drying cycles, the winter season remains a statistically independent hydrological regime.

Table 5: Periodic and non-periodic oscillatory bands regulating multi-scale precipitation variability, including their temporal scales, driving mechanisms, and seasonal impacts.

Oscillatory Band	Time Scale	Primary Driver	Seasonal Impact
Inter-annual	2–4 Years	**ENSO**	High-frequency monsoon/pre-monsoon fluctuations.
Inter-decadal	4–8 Years	**ENSO-IOD Coupling**	Modulation of monsoon onset and retreat.
Decadal	8–16 Years	**Monsoon Variability**	Long-term cycles of wet/dry epochs.
Independent	Non-periodic	**Western Disturbances**	Localized winter precipitation variability.

This intersection suggests that future hydrological shifts will likely manifest as "spectral extremes," where the established 2–4 year cycles become more violent in high-elevation zones. Consequently, water management must evolve from a static model to a dynamic one that accounts for both the predictable periodic rhythms of global climate drivers and the fixed spatial sensitivities of the basin's agroclimatic zones.

Cross-Wavelet Analysis of Inter-Seasonal Precipitation

The cross-wavelet analysis of seasonal rainfall (1985–2022) reveals a highly synchronized, time-frequency dependent structure across the Ganga River basin, primarily within the 1.5–3.5-year periodicity band (Fig. 5). The most robust feature is the persistent coherence between the monsoon and pre-monsoon seasons, particularly within the 2–3-year ENSO-IOD cycle. This coupling, most pronounced in the Upper and Middle Ganga Plains (Zones 1–4), indicates that pre-monsoon convective activity and associated soil-moisture conditioning serve as critical precursors to monsoon onset and intensity. These phase linkages suggest that early-season atmospheric teleconnections, modulated by global climate modes, effectively "prime" the basin for the subsequent monsoon surge.

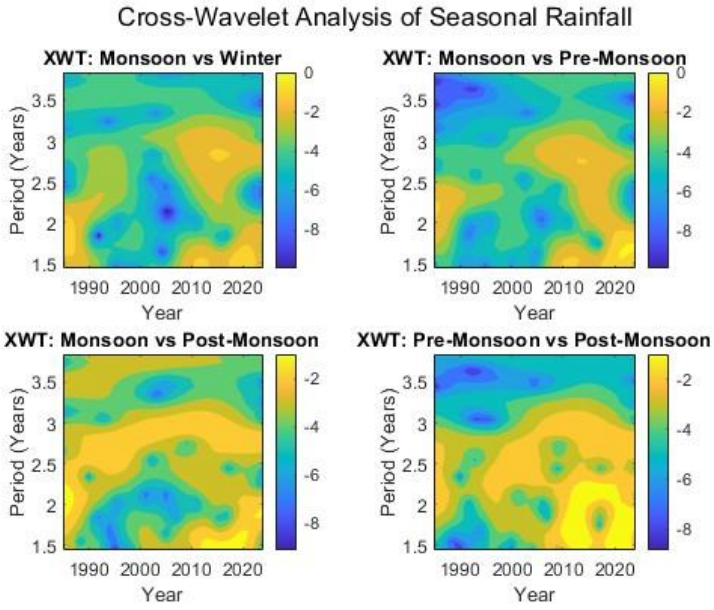
Table 6: Cross-seasonal precipitation coherence and phase couplings within the study domain, detailing periodicity bands, coherence strengths, and dominant atmospheric/surface drivers

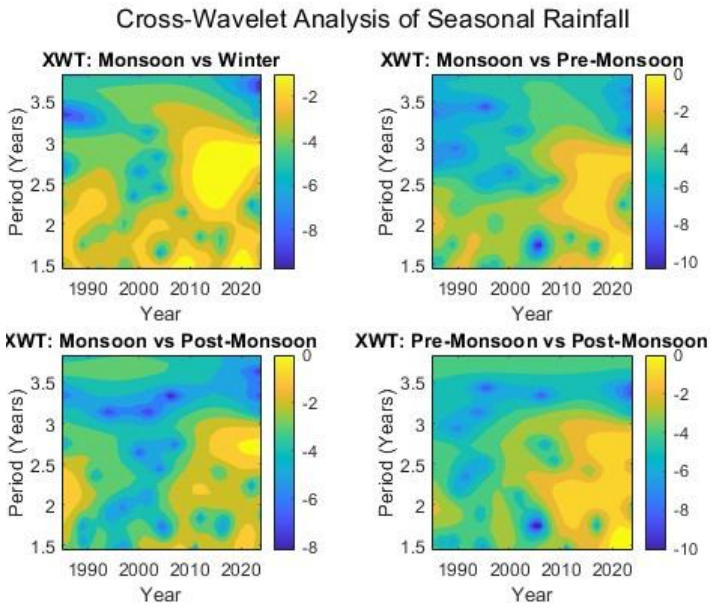
Seasonal Pair	Periodicity Band	Coherence Strength	Dominant Driver
Monsoon – Pre-monsoon	2.0 – 3.0 Years	**High / Persistent**	ENSO/IOD; Soil-moisture conditioning
Monsoon – Post-monsoon	1.5 – 3.5 Years	**Episodic**	Moisture carryover; Monsoon retreat phase
Monsoon – Winter	Variable	**Weak / Sporadic**	Decoupling: Tropical vs. Mid-latitude drivers
Transitional Phases	< 2.0 Years	**Minimal**	Localized convective/thermal instability

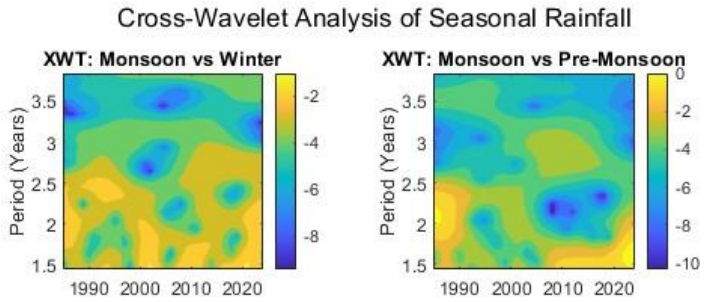
Table :

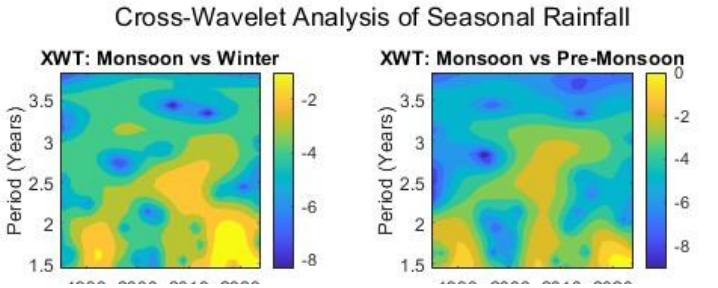
Conversely, the relationship between the monsoon and winter seasons remains weak and sporadic, confirming a fundamental synoptic decoupling. While monsoon variability is dictated by tropical oscillations, winter precipitation is governed by mid-latitude Western Disturbances, creating a distinct hydrological regime. Although occasional coherence was observed in Zones 2, 4, and 7 during 2000–2010 ($2.5–3.5\text{-year}$ cycles), these signals lack long-term persistence, likely representing transient ENSO-related circulation anomalies rather than a stable physical link. Furthermore, intensified high-power clusters in the eastern and deltaic zones (Zones 5–7 and 9–10) during major El Niño events (e.g., 1997–98) and post-2015 IOD shifts underscore the increasing sensitivity of the lower basin to global climate volatility. These findings establish the monsoon–pre-monsoon coherence as the most reliable predictor of inter-annual variability,

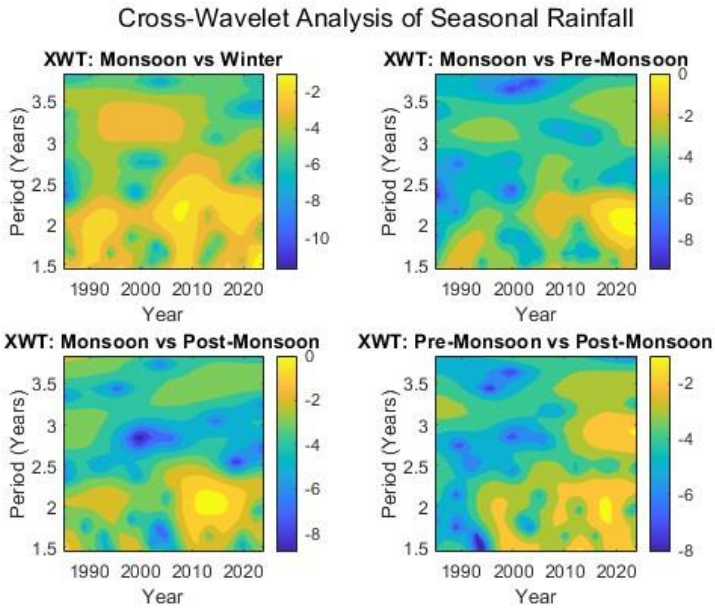
providing a crucial framework for seasonal forecasting and water resource management in this climatically sensitive basin.

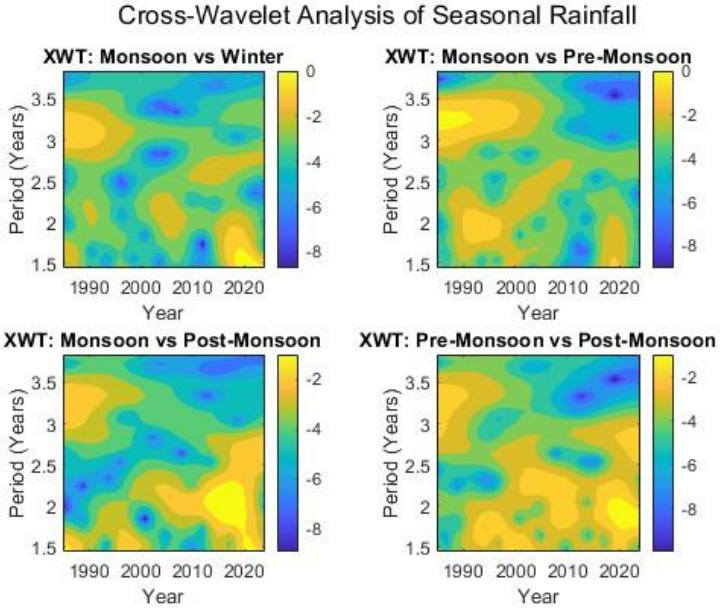












430

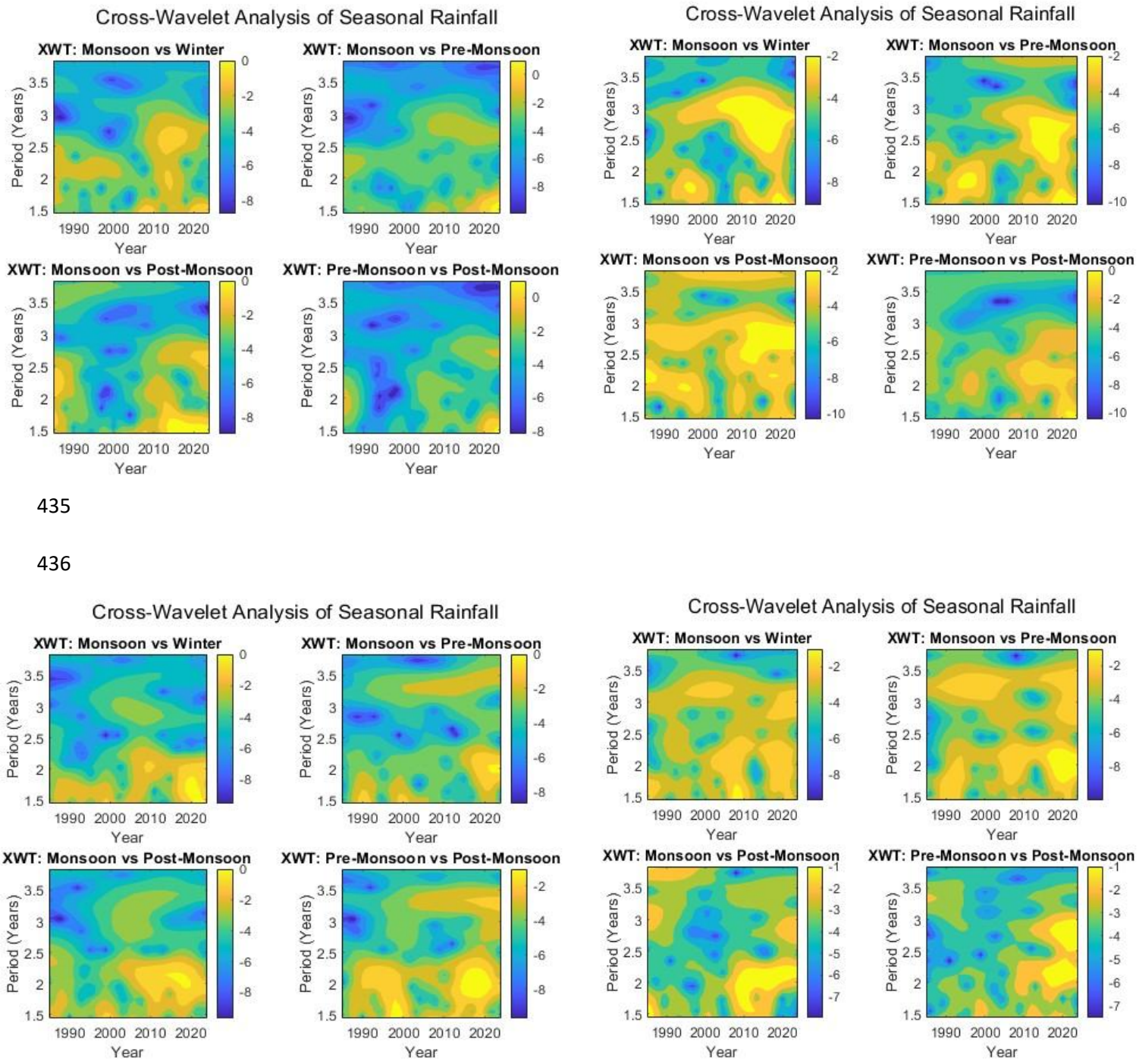


Fig 5: Cross Wavelet Analysis for Inter -Seasonal precipitation over Ganga Basin Zonally

DISCUSSION

Spatial Heterogeneity and Orographic Modulation

The research reveals a fundamental geographic bifurcation in the Ganga River basin's rainfall-elevation relationship. In the Northern Foothills (Zones 1–4), a positive orographic gradient serves as a mechanical intensifier, where uplift drives moisture convergence and increases precipitation with altitude. Conversely, the Eastern Floodplains and Delta (Zones 8–10) exhibit an inverse relationship, with moisture concentrated in low-lying alluvial sinks. This spatial polarization suggests that the basin's topography does not merely distribute water but defines the specific vulnerability of each zone; the extreme contrast in Zone 2—ranging from 0 mm to 2797 mm—proves that regional water management cannot rely on zonal averages but must account for high-resolution topographic heterogeneity.

Temporal Shifts and Seasonality Compression

Long-term analysis (1984–2024) indicates a "progressive wetting" of the basin, yet this volume increase is coupled with diminished hydrological stability. The findings suggest a compression of seasonality, where annual totals are increasingly delivered through high-intensity, short-duration events rather than sustained seasonal rain. This "pulsing" hydrology is evident in the record-breaking 2019 monsoon in Zone 1 (1389 mm). Such volatility disrupts traditional agricultural calendars, as predictable lean and peak periods are replaced by erratic moisture surges, indicating that the basin is shifting toward a regime of unpredictable extremes.

Spectral Periodicities and Global Teleconnections

Wavelet-based spectral analysis identifies the 2–4 year ENSO and 4–8 year ENSO-IOD bands as the dominant drivers of the basin's inter-annual variability. The robust cross-wavelet coherence between pre-monsoon and monsoon seasons—particularly in Zones 1–4—establishes the pre-monsoon as a critical climatic precursor. This synchronization suggests that early-season convective activity effectively "primes" the basin's atmosphere, making pre-monsoon rainfall a statistically significant predictor for monsoon strength. The intensification of high-power clusters after 2015 further indicates an escalating sensitivity to global climate modes across the basin.

Synoptic Decoupling of Winter Systems

A critical finding is the persistent decoupling of winter rainfall from tropical monsoon dynamics. While summer and transitional seasons are governed by ENSO and IOD, winter precipitation remains governed by mid-latitude Western Disturbances. The lack of spectral coherence between winter and the monsoon-dominated seasons confirms that the Ganga basin operates under two independent atmospheric engines. This decoupling is essential for policy, as it implies that water security strategies for the Rabi (winter) season cannot be extrapolated from monsoon trends and require separate, independent forecasting models.

CONCLUSION

This study provides a comprehensive four-decade (1984–2024) assessment of seasonal rainfall variability across the Ganga River Basin (GRB), revealing that the basin's hydrology is governed by a complex nexus of global teleconnections and local physiographic modulators. The analysis identifies a basin-wide "progressive wetting" trend, yet this increase is not spatially or temporally uniform. In the Upper and Middle Gangetic Plains (Z3–Z4), rainfall increases are steady and linked to strengthened monsoon connectivity, whereas the Central Plateau and Lower Gangetic Plains (Z1–Z2) exhibit rising totals punctuated by severe inter-annual fluctuations. These findings suggest that while the basin is becoming wetter, its hydrological stability is being compromised by a "pulsing" regime where annual totals are increasingly delivered through high-intensity extreme events rather than sustained seasonal rain.

Topography and synoptic decoupling emerge as the primary regulators of this spatial distribution. Elevation acts as a force multiplier in the Western Himalayas (Z7) through orographic enhancement, while triggering rain-shadow suppression in low-lying and arid zones like the Western Dry Region (Z10). Wavelet diagnostics further highlight a dominant 2–3-year periodic coherence between pre-monsoon and monsoon rainfall, driven by the 2–4 year ENSO and 4–8 year ENSO-IOD bands. This robust coupling establishes early-season convective activity as a critical climatic precursor to monsoon intensity. Conversely, winter rainfall remains fundamentally decoupled from tropical dynamics, governed instead by mid-latitude Western Disturbances, confirming that the basin operates under two independent atmospheric engines.

Ultimately, the diversity of rainfall behavior across the GRB underscores that "one-size-fits-all" water management is no longer viable. While this study is limited by the static treatment of elevation and the exclusion of land-use variables, it establishes a clear framework for zone-specific

climate adaptation. Future research must integrate high-resolution satellite data and machine learning to refine seasonal forecasting, focusing on the escalating sensitivity to global climate modes observed post-2015. Transitioning to decentralized, climate-resilient strategies that account for both predictable spectral rhythms and localized topographic sensitivities is essential for safeguarding agricultural livelihoods and hydrological security across this climatically sensitive basin.

Conflict of Interest

The authors declare that they have no conflict of interest.

Availability of Data and Materials

The data and materials supporting the findings of this study are available from the corresponding author upon reasonable request.

Author Contributions

Kshitij Divyansh: Conceptualization, methodology, investigation, data collection, analysis, and manuscript preparation. **V. S. Rathore:** Supervision, guidance, critical revision, and review of the manuscript. Both authors read and approved the final manuscript.

References

Abbass, K., et al. (2022). Climate change impacts, adaptation and mitigation: A global assessment. Environmental Science and Pollution Research, 29(47), 70000–70020. https://doi.org/10.1007/s11356-022-19718-6

Acar, R., & Abdourahamane, N. (2018). Continuous wavelet transform analysis in hydrology. Applied Mathematical Modelling, 55, 341–359.

Adarsh, S., Nourani, V., Archana, D. S., & Dharan, D. S. (2020). Multifractal description of daily rainfall fields over India. Journal of Hydrology, 586, 124913. https://doi.org/10.1016/j.jhydrol.2020.124913

Adamowski, J., Abdul-Aziz, O. I., & Chan, H. (2009).-wavelet-based hydrologic signal detection. Water Resources Research, 45, W08426.

Addison, P. S. (2017). The illustrated wavelet transform handbook (2nd ed.). CRC Press. https://doi.org/10.1201/9781315372556

Alemu, G. T., & Dioha, M. O. (2020). Trend detection using Mann–Kendall in rainfall series. Theoretical and Applied Climatology, 141, 677–690.

Amato, F., et al. (2020). Rainfall prediction using neural networks and wavelet transforms. Neural Computing and Applications, 32, 10321–10335.

Banerjee, A., et al. (2024). Performance evaluation of CHIRPS rainfall data for Indian monsoon monitoring. Meteorological Applications, 31(1), e2261. https://doi.org/10.1002/met.2261

Bellard, C., et al. (2012). Vulnerability of biodiversity hotspots to climate change. Global Change Biology, 18, 3015–3027.

Bhutiyani, M. R., et al. (2010). Himalayan climate trend analysis using precipitation series. International Journal of Climatology, 30, 530–540.

Bookhagen, B., & Burbank, D. W. (2010). Toward a complete Himalayan hydrological budget. Journal of Geophysical Research: Earth Surface, 115, F03019. https://doi.org/10.1029/2009JF001426

Bouguettaya, A., et al. (2015). Clustering methods and applications in Earth sciences. Advances in Data Analysis and Classification, 9, 1–25.

Branco, G., et al. (2019). Detecting vegetation change using Theil–Sen and MK tests. Remote Sensing Applications, 15, 100–112.

Caloiro, M. (2014). Rainfall periodicity in Mediterranean basins using wavelets. Water Resources Management, 28, 221–237.

Cerón, W. L., et al. (2020). Spatial classification of rainfall zones using PCA and clustering. Theoretical and Applied Climatology, 142, 1305–1324.

Chavan, P., & Gupta, V. (2021). Seasonal rainfall periodicity using wavelet transforms. Journal of Water and Climate Change, 12, 349–365.

Citakoğlu, H., & Minarecioglu, E. (2021). Hydrological trend analysis under climate variability. Hydrological Sciences Journal, 66, 1019–1031.

Cooley, S. R., & Chang, M. (2021). Identifying precipitation change points using MK tests. Journal of Climate, 34, 3451–3467.

Dimri, A. P., et al. (2015). Western Disturbance dynamics and winter rainfall in India. Climate Dynamics, 44, 2963–2982.

Donat, M. G., et al. (2013). Updated analyses of temperature and precipitation extremes. Journal of Geophysical Research: Atmospheres, 118, 2098–2118.

Everitt, B. S., & Dunn, G. (1991). Applied multivariate data analysis. Oxford University Press.

Ficklin, D. L., et al. (2010). Climate change impacts on watershed hydrology. Hydrological Processes, 24, 1261–1272.

Ghosh, S., et al. (2019). Orographic influences on rainfall distribution in the Eastern Himalayas. Climate Dynamics, 52, 1659–1675.

Gilbert, R. O. (1987). Statistical methods for environmental pollution monitoring. Wiley.

Gupta, V., & Chavan, P. (2021). Assessing rainfall periodicity using wavelet transforms. Journal of Water and Climate Change, 12(1), 349–365.

Haghtalab, N., et al. (2020). Stationarity and trend detection in hydroclimatic time series. Journal of Hydrology, 585, 124779.

Han, Z., et al. (2021). Multi-scale precipitation variability in semi-arid China using wavelet analysis. Climate Dynamics, 57, 2123–2142.

Haktanir, T., & Citakoğlu, H. (2014). Trend tests on maximum rainfall series. Hydrological Sciences Journal, 59(12), 1–14.

Hirsch, R. M., & Slack, J. R. (1987). A nonparametric trend test for seasonally varying data. Water Resources Research, 23(5), 739–742.

Ho, M., et al. (2016). Applications of precipitation trends in hydrology. Hydrology Research, 47, 1000–1015.

Hochman, A., et al. (2019). Identifying multi-scale rainfall variability using wavelets. Climate Dynamics, 53, 345–360.

Hock, R., et al. (2019). Glacier changes and hydrology. In IPCC Special Report on Oceans and Cryosphere.

Hu, Q., et al. (2019). Elevation-dependent precipitation trends in Himalayan regions. Journal of Hydrology, 568, 161–172.

IPCC. (2022). Climate Change 2022: Impacts, adaptation and vulnerability. Cambridge University Press.

Jaya, R., et al. (2022). Regionalization of precipitation using hierarchical clustering. International Journal of Climatology, 42(5), 2567–2582.

Joshi, P., et al. (2016). Detecting rainfall periodicities using Morlet wavelet. Atmospheric Research, 182, 220–233.

Kendall, M. G. (1975). Rank correlation methods (4th ed.). Griffin.

Khadr, M. (2016). Precipitation trend assessment using MK test. Water Resources Management, 30(2), 543–560.

Krishnamurthy, V., & Goswami, B. N. (2000). Indian monsoon–ENSO relationships. Journal of Climate, 13, 579–595.

Li, X., et al. (2021). Multi-scale wavelet analysis of monsoon precipitation. Climate Dynamics, 57, 123–141.

Liu, X., et al. (2016). DWT applications in hydrological time series. Journal of Hydrology, 534, 123–135.

Loucks, D. P., & van Beek, E. (2017). Water resource systems planning and management. Springer.

Machiwal, D., & Jha, M. K. (2019). Regionalization and trend detection in rainfall. Hydrological Sciences Journal, 64(9), 1069–1084.

Mann, H. B. (1945). Nonparametric tests against trend. Econometrica, 13(3), 245–259.

Masson-Delmotte, V., et al. (2022). IPCC Sixth Assessment Report (AR6). Cambridge University Press.

Minarecioglu, E., & Citakoğlu, H. (2021). Trend and homogeneity of rainfall extremes. Atmospheric Research, 256, 105592.

606 Moradian, S., & Yazdandoost, F. (2021). Climate change impacts on hydrology: A global review.
607 Journal of Environmental Management, 285, 112060.

608 Nalley, D., Adamowski, J., & Khalil, B. (2012). Integrating wavelets with machine learning for
609 hydrology. Journal of Hydrologic Engineering, 17(10), 1080–1092.

610 Oppenheimer, M., et al. (2019). IPCC Special Report on Ocean and Cryosphere.

611 Orkodjo, Z., et al. (2022). Climate change and rainfall intensity shifts. Nature Climate Change, 12,
612 1120–1128.

613 Pai, D. S., et al. (2020). Indian monsoon onset and variability. Journal of Climate, 33, 9325–9343.

614 Palizdan, N., et al. (2017). Rainfall modeling using wavelet methods. Journal of Hydrology, 545,
615 22–34.

616 Panda, D., & Sahu, N. (2019). Rainfall variability in Indian basins. Atmospheric Research, 220,
617 111–121.

618 Panda, D., et al. (2023). Shifting monsoon patterns in India. Climate Dynamics, 60, 119–138.

619 Pandey, R. P., et al. (2017). Wavelet–statistical technique for rainfall trend detection. Journal of
620 Hydrology, 553, 155–170.

621 Pathak, A., et al. (2016). Wavelet-based rainfall periodicity analysis. Hydrological Processes, 30,
622 1023–1036.

623 Pradhan, R. K., et al. (2019). Climate variability and precipitation shifts. International Journal of
624 Climatology, 39, 4201–4214.

625 Praveen, V., et al. (2020). Spatial heterogeneity in the Indian monsoon. Climate Dynamics, 54,
626 4317–4334.

627 Rashid, M., et al. (2015). Multi-temporal rainfall analysis using CWT. Theoretical and Applied
628 Climatology, 122, 415–428.

629 Rehman, S., et al. (2022). Hydrological extremes and climate change. Environmental Research,
630 212, 113321

631 Reddy, M. J., & Adarsh, S. (2016). Wavelet-based analysis of Indian hydroclimatic variability.
632 Journal of Hydrology, 535, 1–15.

633 Riabova, L. (2018). Wavelet applications in hydrology: State of the art. Water Resources
634 Management, 32, 4599–4612.

635 Rousseeuw, P. J. (1987). Silhouettes in cluster analysis. Journal of Computational and Applied
636 Mathematics, 20, 53–65.

637 Roy, T., et al. (2020). Orographic rainfall enhancement across the Himalayas. Climate Dynamics,
638 54, 567–585.

639 Ruwangika, S., et al. (2020). Wavelet-based variability of rainfall in monsoon regions.
640 Meteorological Applications, 27, e1903.

641 Sahu, N., et al. (2019). Variability in India's monsoon rainfall. Climate Dynamics, 52, 2163–2176.

642 Sang, Y. F. (2013). A review of wavelet methods in hydrology. Atmospheric Research, 122, 31–
643 43.

644 Schmidt, J., et al. (2019). Regionalizing hydroclimatic variables using EOF and PCA. Journal of
645 Hydrology, 575, 1112–1132.

646 Sen, P. K. (1968). Estimates of the regression coefficient based on Kendall's tau. Journal of the
647 American Statistical Association, 63(324), 1379–1389.

648 Sharma, S., et al. (2018). Monsoon variability under climate change. Climate Dynamics, 50, 3645–
649 3661.

650 Shrestha, N. K., et al. (2017). Evaluation of CHIRPS rainfall data for the Indian region. Journal of
651 Hydrology: Regional Studies, 13, 220–234.

652 Singh, D., et al. (2017). Orographic effects on Himalayan precipitation. Climate Dynamics, 48,
653 1903–1920.

654 Srivastava, A., et al. (2021). Seasonal rainfall variability and drought assessment in India. Journal
655 of Hydrology, 595, 126040.

656 Tabari, H. (2020). Climate change impacts on precipitation extremes. Atmospheric Research, 240,
657 104911.

658 Theil, H. (1950). Rank-invariant regression analysis. Nederl. Akad. Wetensch. Proc., 53, 386–392.

Torrence, C., & Compo, G. P. (1998). Practical guide to wavelet analysis. Bulletin of the American Meteorological Society, 79, 61–78.

Torrence, C., & Webster, P. J. (1999). ENSO–monsoon system variability. Journal of Climate, 12, 2679–2690.

van der Wiel, K., & Bintanja, R. (2021). Climate-driven precipitation variability. Communications Earth & Environment, 2, 1–11.

Wang, W., et al. (2020a). Improving MK trend tests under serial correlation. Advances in Water Resources, 136, 103498.

Ward, J. H. (1963). Hierarchical grouping method. Journal of the American Statistical Association, 58, 236–244.

Yang, X., et al. (2019). Theil–Sen slope and precipitation dynamics. Hydrological Processes, 33, 1325–1337.

Yao, T., et al. (2016). Glacier and hydrological changes in the Himalayas. Nature Climate Change, 6, 169–174.

Yerdelen, C., et al. (2021). Wavelet-based drought periodicity. Journal of Arid Environments, 188, 104457.

Zerouali, B., et al. (2020). Hybrid ANN–wavelet rainfall forecasting. Neural Computing & Applications, 32, 15567–15584.

Zhu, Y., et al. (2010). Silhouette validation for cluster number selection. Pattern Recognition Letters, 31, 2225–2236.

Zhu, Y., et al. (2020). Multi-scale variability of monsoon rainfall. International Journal of Climatology, 40, 3210–3226.

Zilli, M., et al. (2017). Climate trend detection with MK test in hydrological series. Climate Dynamics, 48, 2685–2702.